Theoretical and Experimental Insights into the Mechanism of the Nucleophilic Addition of Water and Methanol to Dicyanonitrosomethanide

ARTICLE *in* THE JOURNAL OF PHYSICAL CHEMISTRY B · NOVEMBER 2010

Impact Factor: 3.3 · DOI: 10.1021/jp108550z · Source: PubMed

Theoretical and Experimental Insights into the Mechanism of the Nucleophilic Addition of Water and Methanol to Dicyanonitrosomethanide

Ekaterina I. Izgorodina,* Anthony S. R. Chesman, David R. Turner, Glen B. Deacon, and Stuart R. Batten

School of Chemistry, Monash University, Wellington Road, Clayton VIC 3800, Australia

Received: September 8, 2010; Revised Manuscript Received: October 29, 2010

In this work the nucleophilic addition of water and methanol to the dicyanonitrosomethanide anion (dcnm, $[C(CN)_2(NO)]^-$) in the absence of the usual transition metal promoters was investigated. Experimentally it was shown that a quantitative conversion of the dcnm anion to carbamoylcyanonitrosomethanide (ccnm, $[C(CN)(CONH_2)(NO)]^-$) by the addition of 1 equiv of water to a nitrile group is complete in 48 h at 100 °C, or in 1.5 h at 150 °C when the reaction is conducted in a microwave reactor. Attempts to add a second equivalent of water to the anion failed with thermal degradation of the anion occurring at 200 °C. *Ab initio* calculations show that the reaction proceeds via three distinct transition states: (1) the transfer of a proton from a water molecule to the nitrile group, (2) the subsequent attack of the generated hydroxide anion on the carbon atom of the nitrile group, and (3) a rapid proton transfer to form a carbamoyl group. The attacking water molecule is shown to be a stronger proton donor when modeled as part of a hydrogen-bonded three water molecule chain, leading to a significant reduction in the reaction barrier. Only the *anti*-ccnm anion is formed in the reaction. There is a high-energy barrier to the formation of the *syn* isomer by the rotation of the nitroso group. While the *syn* isomer of ccnm is shown to be the more thermodynamically stable conformation, examination of the HOMO−1 molecular orbital that arises during the second transition state of the reaction indicates the addition of the hydroxide anion to the carbon atom is forbidden due to orbital symmetry, with a similar effect responsible for the failure of a second equivalent of water to add to the ccnm anion. Under analogous reaction conditions the addition of 1 equiv of methanol to dcnm to form cyano(imino(methoxy)methyl)nitrosomethanide (cmnm, $[C(CN)(C(OMe)NH)(NO)]^-$) failed, although *ab initio* calculations initially indicated the reaction should proceed more readily than the addition of water. When the energy required to break the hydrogen-bonded cyclic hexamers in methanol is taken into consideration, the energy barrier to the first transition step is greatly increased. The addition of a second equivalent of methanol to cmnm is unlikely to occur even in the presence of a transition metal as the resultant anion would be marginally thermodynamically unstable.

Introduction

The unique properties of polynitrile methanides make them ideal for inclusion in a range of materials. While the anions dicyanamide (dca, $[N(CN)_2]^-$) and tricyanomethanide (tcm, $[C(CN)_3]^-$) have long garnered attention for their propensity to form coordination polymers that display a wide variety of magnetic properties,[1] they have more recently found application as anions in ionic liquids (ILs).[2−14] As with the newly developed polynitroso- and polynitromethanides,[15−17] polynitrile methanides contain electron withdrawing functional groups giving rise to resonance-stabilized planar species with highly delocalized anionic charges,[18] rendering them ideal for inclusion in ionic liquids.[19]

The dca and tcm anions, along with the related carbamoyldicyanomethanide anion (cdm, $[C(CN)_2(CONH_2)]^-$), readily undergo nucleophilic addition to a nitrile group, providing a convenient means of in situ ligand synthesis in the formation of transition metal complexes.[20−26] The dicyanonitrosomethanide anion (dcnm, $[C(CN)_2(NO)]^-$)[27−29] has been demonstrated to have an even greater propensity to undergo this reaction. For the dcnm anion, the reaction has been shown to occur under three distinct sets of conditions: (1) in the presence of a transition metal, which may promote the addition of water, an alcohol or an amine,[30−40] (2) in the presence of an acid, which may promote the addition of an amine,[41−43] or (3) by heating an aqueous reaction solution containing the dcnm anion with a nonmetallic countercation to reflux, which has been shown to result in the addition of water, giving the carbamoylcyanonitrosomethanide anion (ccnm, $[C(CN)(CONH_2)(NO)]^-$), as shown in Figure 1.[44]

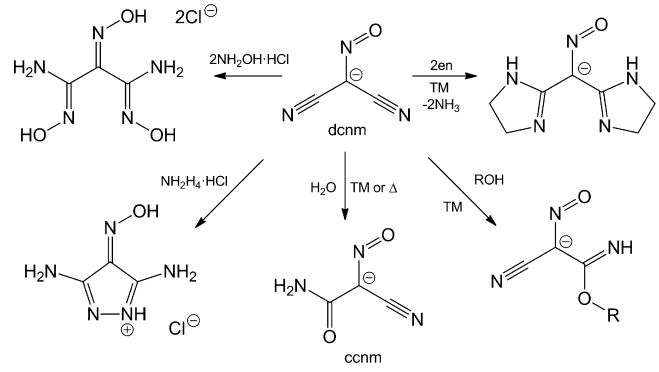

Figure 1. Products resulting from the transition metal or acid promoted addition of nucleophiles to the dcnm anion (ROH = methanol, ethanol, and ethylene glycol monomethyl ether).

* Corresponding author. E-mail: Katya.Izgorodina@monash.edu.

10.1021/jp108550z
Published on Web 11/18/2010

Despite numerous literature reports, certain aspects of this reaction are yet to be adequately understood, namely why the addition of an amine may occur to both of the nitrile groups of the dcnm anion while water or alcohols have been observed to react only with one nitrile group. Furthermore, when only one nitrile group has reacted, the resultant anion is predominantly the *anti* isomer, rather than the *syn* isomer. The particular isomer formed can greatly affect the properties of an anion, as described for the closely related cyanoximate anions[45−50] where the nature of the isomer can be responsible for the biological activity.[51,52]

Previous studies of polynitrile methanides have used nucleophilic addition in the presence of transition metal ions as means of in situ ligand synthesis. In this study we investigate whether the nucleophilic addition of water and methanol to the dcnm anion can occur as easily without transition metal cations. The reactivity of the dcnm anion to solvent was probed through a series of reactions in which an aqueous or methanolic solution of (Me_4N)(dcnm) was heated by either microwave or conventional means. X-ray crystallography and ^{13}C NMR spectroscopy were used in concert to determine the isomer formed.

Although the thermodynamic stability of cyano-, nitro-, and nitrosomethane derivatives has been studied using the density functional theory methods,[18,53] no theoretical study on the mechanism of the nucleophilic addition of water and methanol to the CN triple bond has been performed so far. In this work a systematic *ab initio* study was also conducted to provide theoretical insight into the mechanism of such additions to the dcnm anion. Reaction enthalpies as well as corresponding reaction barriers in the gas phase and in water and methanol were calculated for the step-by-step addition of water and methanol molecules to the two available nitrile groups of the dcnm anion. High correlated levels of *ab initio* theory, such as MP2 and CCSD(T), in combination with the aug-cc-pVTZ basis set were employed to calculate thermodynamics and kinetics of the nucleophilic addition. Solvent effects were calculated by means of the COSMO and COSMO-RS models that explicitly consider hydrogen bonding interactions between the solute and solvent. In this study we have resolved the existing ambiguity in the literature regarding two issues: (1) which nitrile arm undergoes the nucleophilic attack first and (2) the ability of the nitroso group in the parental dcnm anion to freely rotate in aqueous solution. We have also studied the effect of two- and three-molecule chains of water and methanol on the mechanism of the nucleophilic addition to the nitrile group.

Experimental Section

General Information. Laboratory reagents and solvents were used as provided commercially. Elemental analyses (C, H, N) were performed by the Campbell Analytical Laboratory, University of Otago, New Zealand. ATR-IR spectra were recorded on a Bruker Equinox 55 series FTIR spectrometer in the range 4000−500 cm^{-1} with a resolution of 4 cm^{-1}. ^{13}C NMR spectra were recorded on in D_2O, MeOD, or DMSO-d_6 on a Bruker Avance 400 (9.4 T magnet) with a 5 mm broad-band autotunable probe with Z-gradients and BACS 60 tube autosampler spectrometer (operating at 100.6 MHz). Microwave reactions were performed in a CEM Discover System. (Me_4N)(dcnm) and Ag(ccnm) were prepared according to literature methods.[29,54]

Synthesis of (Me_4N)(ccnm). (Me_4N)(dcnm) (300 mg, 1.78 mmol) was dissolved in water (50 mL) and heated under reflux for 48 h. The reaction solution was allowed to cool to room temperature before the solvent was removed under reduced pressure. The yellow powder of (Me_4N)(ccnm) was dried under high vacuum for three hours. ^{13}C NMR indicates the presence of both *anti* and *syn* isomers (^{13}C NMR (100.6 MHz, D_2O): δ 55.3 (Me_4N^+), 112.2 (*anti*-C≡N), 118.8 (*syn*-C≡N), 129.0 (*anti*-C—NO), 133.5 (*syn*-C—NO), 161.0 (*syn*-$CONH_2$), 167.1 (*anti*-$CONH_2$)). (Figure S1a, Supporting Information). The bulk material was dissolved in methanol and acetone, with a diethyl ether diffusion into the solution yielding X-ray quality crystals of the *anti* isomer of (Me_4N)(ccnm) in 3 days. The product is hygroscopic and was submitted for elemental analysis in a sealed ampule under an atmosphere of nitrogen. Yield: 75 mg, 23%. Anal. Calcd for $C_7H_{14}N_4O_2$ (186.21): C 45.16, H 7.58, N 30.09. Found: C 45.09, H 7.77, N 29.91. IR (ATR), cm^{-1}: 3440 (m), 3305 (w), 3243 (w), 3166 (s), 3031 (w), 2959 (vw), 2828 (vw), 2197 (m), 1647 (s), 1585 (m), 1486 (s), 1423 (m), 1344 (m), 1253 (s), 1160 (m), 1092 (w), 950 (m), 780 (w), 697 (w). ^{13}C NMR (100.6 MHz, D_2O): δ 55.2 ((Me_4N^+), 112.2 (*anti*-C≡N), 129.0 (*anti*-C—NO), 167.2 (*anti*-$CONH_2$) (Figure S1b, Supporting Information).

Alternate Synthesis of (Me_4N)(ccnm). (Me_4N)(dcnm) (50 mg, 297 μmol) was dissolved in water (4 mL), and the solution was heated in the microwave reactor at 150 °C for 1.5 h. The water was removed under vacuum, leaving a yellow powder, which was identified by ^{13}C NMR spectroscopy to be (Me_4N)(ccnm). ^{13}C NMR (100.6 MHz, D_2O): δ 55.3 (Me_4N^+), 112.3 (*anti*-C≡N), 119.0 (*syn*-C≡N), 128.9 (*anti*-C—NO), 133.6 (*syn*-C—NO), 161.0 (*syn*-$CONH_2$), 167.2 (*anti*-$CONH_2$)).

Study of the Conversion of *anti*-ccnm to *syn*-ccnm by ^{13}C NMR Spectroscopy. Three separate solutions were prepared by dissolving crystals of (Me_4N)(*anti*-ccnm) (30 mg, 161 μmol) in D_2O, MeOD-d_4 or DMSO-d_6 (1 mL). A ^{13}C NMR spectrum was collected for each solution 1, 24, and 96 h after dissolution. ^{13}C NMR (100.6 MHz, D_2O) after 1 h: δ 55.2 (Me_4N^+), 112.2 (*anti*-C≡N), 129.0 (*anti*-C—NO), 167.2 (*anti*-$CONH_2$). No change after 96 h (Figure S3, Supporting Information). ^{13}C NMR (100.6 MHz, MeOD-d_4) after 1 h: δ 56.0 (Me_4N^+), 113.7 (*anti*-C≡N), 129.5 (*anti*-C—NO), 168.6 (*anti*-$CONH_2$). No change after 24 h, appearance of small peak at 121.5 (*syn*-C≡N) after 96 h (Figure S4, Supporting Information). ^{13}C NMR (100.6 MHz, DMSO-d_6) after 1 h: δ 54.4 (Me_4N^+), 115.3 (*anti*-C≡N), 127.9 (*anti*-C—NO), 167.4 (*anti*-$CONH_2$). Appearance of small peaks at 134.2 (*syn*-C—NO), 160.0 (*syn*-$CONH_2$) after 24 h, appearance of small peak at 121.9 (*syn*-C≡N) after 96 h (Figure S5, Supporting Information).

Crystals of (Me_4N)(*anti*-ccnm) (35 mg, 188 μmol) were dissolved in D_2O (1.5 mL). ^{13}C NMR (100.6 MHz, D_2O): δ 55.2 (($(CH_3)_4N^+$), 112.1 (*anti*-C≡N), 129.0 (*anti*-C—NO), 167.2 (*anti*-$CONH_2$). This solution was directly added to water (20 mL), and the resultant solution heated at reflux for 48 h. Cooling to room temperature and evaporation of the solvent under reduced pressure gave (Me_4N)(ccnm) as a yellow powder, which was dried under vacuum for 3 h. ^{13}C NMR (100.6 MHz, D_2O): δ 55.3 (Me_4N^+), 112.1 (*anti*-C≡N), 118.9 (*syn*-C≡N), 129.0 (*anti*-C—NO), 133.5 (*syn*-C—NO), 161.1 (*syn*-$CONH_2$), 167.2 (*anti*-$CONH_2$).

Attempted Synthesis of (Me_4N)(dccm) (dccm = di(carbamoyl)nitrosomethanide). A solution of (Me_4N)(dcnm) (200 mg, 1.1.89 mmol) dissolved in water (4 mL) was heated at 200 °C for 1.5 h in the microwave reactor. The initially deep yellow solution turned a very light yellow color. Mass spectrometry indicated the presence of degradation products and a trace of the ccnm anion. No mass ion peak corresponding to the dccm was present in the spectrum. ESI-(MS^-): 45.0 (100%, $C_2H_5O^-$), 75.0 (15%, $C_2H_7N_2O^-$), 112.0 (5%, ccnm).

Attempted Synthesis of (Me_4N)(cmnm). A solution of (Me_4N)(dcnm) (100 mg, 595 μmol) dissolved in MeOH (4 mL)

was heated at 150 °C for 5 h in the microwave reactor. Mass spectrometry indicated the presence of degradation products with a trace of the cmnm anion. The dcnm anion was the predominant anion detectable in solution. ESI-(MS^-): 42.1 (20%, CNO^-), 94.0 (100%, dcnm), 126.0 (10%, cmnm), 262.1 (10%, $[(Me_4N)(dcnm)_2]^-$).

Crystallography. A crystal was mounted on a fine glass fiber using viscous hydrocarbon oil. Data were collected on a Nonius Kappa-CCD diffractometer equipped with graphite monochromated Mo Kα radiation ($\lambda = 0.710\ 73$ Å). The data collection temperature was maintained at 173 K using an open flow N_2 cryostream. Data integration was carried out by the program DENZO-SMN and data were corrected for Lorentz-polarization effects and for absorption using the program SCALEPACK.[55] An initial solution was obtained by direct methods using SHELXS-97[56] followed by successive refinements using full matrix least-squares methods against F^2 using SHELXL-97.[56] The program X-Seed was used as a graphical SHELX interface.[57] Hydrogen atoms attached to carbon atoms were placed in idealized positions and refined against a riding model to the atom to which they are attached. All non-hydrogen atoms were refined anisotropically.

Crystal Data. $(Me_4N)(ccnm)$: $C_7H_{14}N_4O_2$, $M = 186.22$, yellow plate, $0.20 \times 0.20 \times 0.10$ mm^3, monoclinic, space group $P2_1/n$ (No. 14), $a = 6.4198(2)$, $b = 17.1798(6)$, $c = 9.5355(3)$ Å, $\beta = 107.353(2)°$, $V = 1003.81(6)$ Å^3, $Z = 4$, $D_c = 1.232$ g/cm^3, $F_{000} = 400$, $2\theta_{max} = 55.0°$, 28 580 reflections collected, 2310 unique ($R_{int} = 0.1143$). Final $GooF = 1.047$, $R1 = 0.0684$, $wR2 = 0.1641$, R indices based on 1454 reflections with $I > 2\sigma(I)$ (refinement on F^2), 122 parameters, 0 restraints, $\mu = 0.093$ mm^{-1}.

Theoretical Procedures. Standard *ab initio* molecular orbital theory and density functional theory (DFT) calculations were carried out using the GAUSSIAN 09[58] and ADF 2009[59] sets of programs. All geometry optimizations were performed at the B3LYP[60,61]/6-31+G(d)[62,63] level of theory. Individual anions were fully conformationally screened (by rotation around the single bonds) at this level of theory to ensure the lowest energy conformations on the potential energy surfaces. Improved electronic energies for the first addition of water and methanol to the dcnm anion were obtained at the CCSD(T)[64]/aug-cc-pVTZ[65,66] level of theory, which is considered the benchmark method in *ab initio* theory.[67] Due to high computational cost, improved energies for the second addition of water and methanol to the ccnm and cmnm anions were calculated at a more feasible correlated level of theory, MP2[68,69]/aug-cc-pVTZ. Free energies of solvation in aqueous solution were calculated using the COMSO-RS approach[70,71] as implemented in the ADF 2009 set of programs. The gas phase transition states were optimized at the MP2/aug-cc-pVDZ level of theory using the Berny algorithm as implemented in GAUSSIAN 09. Improved reaction barriers were calculated at the MP2/aug-cc-pVTZ level of theory in the gas phase and in solvent (either water or methanol) using the COSMO model as implemented in GAUSSIAN 09. The COSMO model represents a conductor-like polarizable continuum model, in which a solute is embedded into a cavity that is surrounded by a dielectric continuum of a certain dielectric constant (e.g., for water the dielectric constant of 80 is taken).[72] Inside the cavity the dielectric constant is considered to be that of vacuum. It has to be noted here that the COSMO model used here accounts only for the Coulomb (electrostatic) component of the overall interaction between the solute and the solvent. Dispersion interactions such as hydrogen bonding are not considered. For consistency, the B3LYP lowest energy conformations of the dcnm anion, water and methanol were reoptimized at the MP2/aug-cc-pVDZ level of theory when the reaction barriers were computed. NMR calculations were performed on optimized geometries at the B3LYP/cc-pVDZ level of theory using the standard GIAO approach.[73,74] Natural bond orbital (NBO) analysis[75,76] was performed at the HF/aug-cc-pVTZ level of theory. Rotational barriers of the NO group in the dcnm and ccnm anions in two of the solvents used in the experiment, water and DMSO, were calculated using relaxed scans with the step of 10 degrees and the COMSO solvation model at the BLYP/TZP level of theory in ADF 2009.

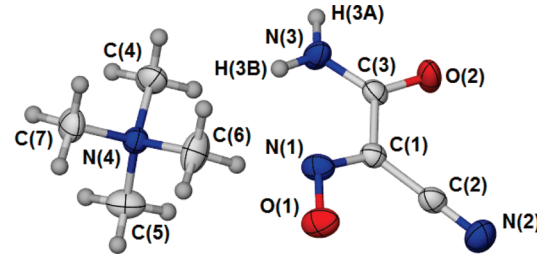

Figure 2. Asymmetric unit from the crystal structure of the *anti* isomer of $(Me_4N)(ccnm)$. Selected bond lengths (Å): N(1)−O(1), 1.293(2); N(1)−C(1), 1.333(3); C(1)−C(2), 1.428(3); C(2)−N(2), 1.150(3); C(1)−C(3), 1.474(3); C(3)−O(2), 1.235(3); C(3)−N(3), 1.325(3).

TABLE 1: Calculated and Observed ^{13}C NMR Shifts (in ppm) for the *Anti* and *Syn* Isomers of ccnm in $(Me_4N)(ccnm)$

	anti isomer		*syn* isomer	
carbon	calculated	observed	calculated	observed
carbamoyl	165.0	167.1	153.4	161.0
methanide	130.5	128.8	136.0	133.5
nitrile	110.6	112.2	119.0	118.9
Me_4N^+		55.2		55.2

Results and Discussion

Water Addition. ***First Water Addition.*** A solution of $(Me_4N)(dcnm)$ dissolved in water was heated under reflux for 48 h. After cooling, the solvent was removed under reduced pressure, to yield $(Me_4N)(ccnm)$, resulting from the nucleophilic addition of one molecule of water to a nitrile group of the dcnm anion. The ^{13}C NMR spectrum of the product contained two sets of signals, indicating that both the *anti* and *syn* isomers of the ccnm anion (termed *anti*-ccnm and *syn*-ccnm, respectively) were present (Figure S1a, Supporting Information). Vapor diffusion of diethyl ether into a solution of the bulk product in methanol and acetone yielded crystals of (Me_4N)(*anti*-ccnm) (Figure 2). The ^{13}C NMR spectrum of the crystals dissolved in D_2O contained a set of peaks due to the presence of a single isomer (Figure S1b, Supporting Information). Calculations of the ^{13}C NMR chemical shifts confirmed the assignment of the peaks and were in good agreement with the experimental data (Table 1).

There are three possibilities as to why both geometric isomers form during the initial reaction: (1) the nucleophilic addition of water may occur to either nitrile group, (2) the addition only occurs to one nitrile group and there is rotation around the C−NO bond of the ccnm anion, or (3) a combination of both. The last two possibilities could not be readily eliminated as a ^{13}C NMR spectrum of an aqueous solution of the *anti* isomer of $(Me_4N)(ccnm)$, which had been heated at reflux for 48 h, revealed a partial conversion to the *syn* isomer had taken place. This suggests that rotation around the C−NO bond may occur, albeit slowly enough for both isomers to observed on the ^{13}C NMR time scale.

This is in contrast to the reported rotational properties of disubstituted arylcyanoxime species.[45] While in the oxime form they demonstrate no conversion between *anti* and *syn* isomers but, upon deprotonation to form the nitroso derivative, there is only one observed set of signals in the ^{13}C NMR spectrum, suggesting free rotation around the C−NO bond. The difference between ^{13}C NMR spectra of the nitroso form of the disubstituted arylcyanoxime species and the ccnm anion may result from greater degree of resonance stabilization in the ccnm anion, increasing the energy barrier for the rotation around the C−NO bond and consequently reducing the rate of the rotation so it can be observed on the ^{13}C NMR time scale. Similarly, the related 2-cyano-2-isonitroso-*N*-morpholinylacetamide species show two sets of signals in the ^{1}H NMR and ^{13}C NMR spectra due to the presence of both the *syn* and *anti* isomers, while the potassium salt of the anionic form only shows one set of signals, attributed to free rotation of the nitroso group and not a single *anti* or *syn* isomeric form.[49]

Computation Study of the Rotation of the Nitroso Group in the dcnm and ccnm Anions. In our NMR measurements distinct ^{13}C chemical shifts were observed for both *anti* and *syn* isomers of the ccnm anion, suggesting restricted rotation of the NO group. Roohi et al.[77] have reported that the nitroso group rotation around the N−N bond in six-membered cyclic nitrosamine compounds was 96 kJ mol^{-1}, calculated at the MP2/6-31G** level of theory, making this rotation energetically restricted. An analogous study by the same authors[78] at the B3LYP/6-31G* level of theory for five-membered cyclic nitrosamines showed that the Gibbs free energy of the nitroso rotation around the N−N bond varied from 51 to 112 kJ mol^{-1}, with the high energy required for the rotation of the nitroso group further supporting the hypothesis of restricted rotation in the dcnm and ccnm anions.

In this study the nitroso group rotation was performed in water for the parent dcnm anion as well as the *anti*-ccnm anion. The rotational barriers calculated in aqueous solution are presented in Figure 3 in the form of relative energies with respect to their minimum-energy geometries. In both cases the rotational barriers are about 155 kJ mol^{-1}, with the highest energy on the graph corresponding to the NO group being perpendicular to the $C(CN)_2$ plane for the dcnm anion, or the $C(CN)(CONH_2)$ plane for the ccnm anion. The steep slopes of the rotational curves reflect a drastic change in the electronic distribution through disruption of the π-conjugated system. This effect may be observed in the dcnm anion when the $[C(CN)_2]$ moiety loses its planarity as the NO group is rotated by 90°. The high rotational barriers were further supported by the natural bond order analysis that confirmed strong electron delocalization in the anions (for more detail see Table S1, Supporting Information).

While the 180° rotation of the NO group in dcnm is predicted to be energetically very demanding, and does not occur instantaneously, it cannot be monitored by ^{13}C NMR spectroscopy as the rotation does not result in the transformation of the anion into a different conformation, and consequently the spectrum of the dcnm anion does not change.

In contrast, the ^{13}C NMR spectra for the *anti* and *syn* isomers of the ccnm anion are distinct, and the calculated sets of chemical shifts for each conformation were confirmed by our experimental ^{13}C NMR measurements. However, conversion of only a small amount of the *anti* isomer to the *syn* isomer is observed, and this can again be attributed to restricted rotation of the nitroso group. This rotation could potentially occur at a lower barrier if the ccnm anion is stabilized by a solvent through

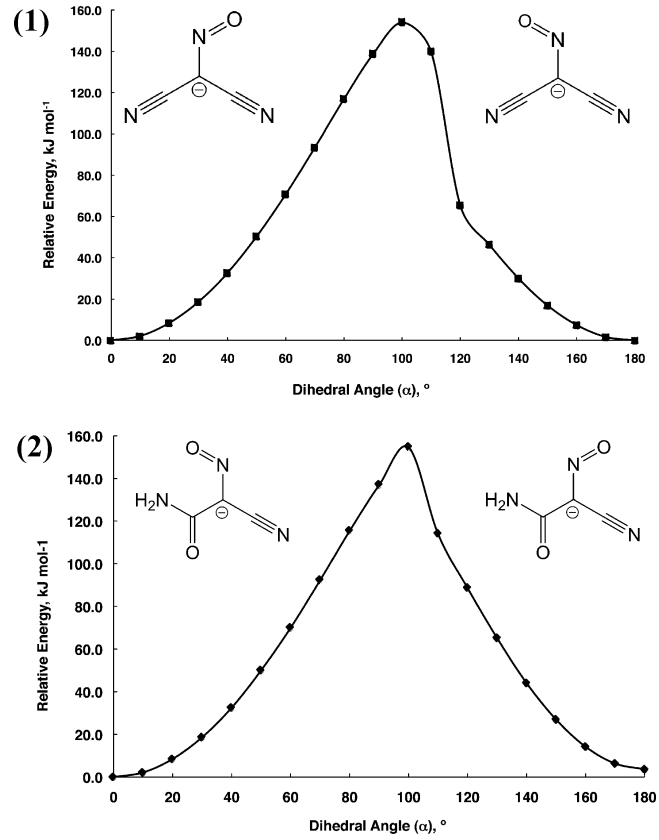

Figure 3. Rotational energy barriers of the nitroso group rotation in (1) the dcnm anion and (2) the ccnm anion.

strong hydrogen bonding or $\pi-\pi$ stacking interactions. Further ^{13}C NMR studies suggest that the rotation of this bond may occur at room temperature, albeit slowly, depending on which solvent (Me_4N)(ccnm) is dissolved in. While the ^{13}C NMR spectrum of crystals of the *anti* isomer of (Me_4N)(ccnm) dissolved in D_2O showed no rotation to the *syn* isomer in 96 h (Figure S3, Supporting Information), samples dissolved in MeOD-d_4 and DMSO-d_6 showed a limited degree of conversion to the *syn* isomer over the same period of time (Figures S4 and S5, Supporting Information). Our calculations of the NO group rotation in the dcnm anion in DMSO-d_6 showed that the rotational barrier is reduced to 138 kJ mol^{-1}, in line with experimental observation.

Reaction Enthalpies: First Water Addition. Optimized geometries of the lowest energy conformations are given in Figure 4. The *anti* and *syn* isomers of the ccnm anion were found to be the two lowest energy conformations. Due to the presence of hydrogen bonding between the oxygen atom of the nitroso group and the NH_2 group in the ccnm anion, the *syn* isomer is more thermodynamically stable by 5 kJ mol^{-1} (as calculated at the B3LYP/6-31+G(d) level of theory). Alternate conformations of the ccnm anions, in which the carbonyl group is adjacent to the nitroso group, are energetically less favorable than the conformations given in Figure 4 (28 and 47 kJ mol^{-1} less thermodynamically stable than the *anti* and *syn* isomers, respectively) and are consequently not expected to form. The reaction enthalpies of the first and second addition of water to the dcnm anion are given in Table 2. Values for the first water addition for the formation of *anti* and *syn* isomers differ by only 8 kJ mol^{-1} in the gas phase. Inclusion of solvent effects makes the difference in the reaction enthalpies within the error of the CCSD(T) calculations, i.e., less than 1 kcal mol^{-1}. From the thermodynamic point of view, the reaction enthalpies do

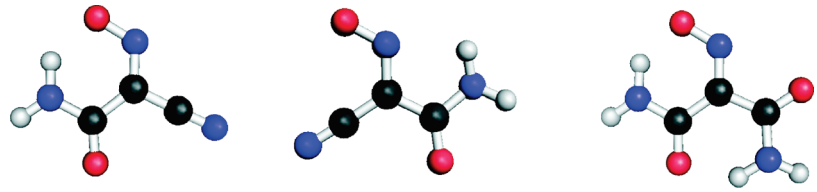

***syn*-ccnm** ***anti*-ccnm** **dccm**

Figure 4. B3LYP/6-31+G(d) gas phase optimized structures of the water addition products (dccm = dicarbamoylnitrosomethanide).

TABLE 2: Reaction Enthalpies (in kJ mol^{-1}) of Water Addition Calculated at the CCSD(T)/aug-cc-pVTZ Level of Theory

Reaction	ΔH_{gas}[a]	ΔH_{solv}[b]
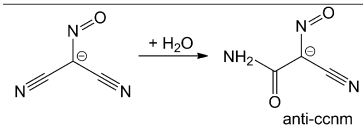	−60.9	−66.0
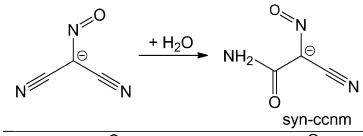	−68.9	−68.1
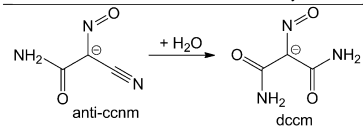	−33.9	−37.6
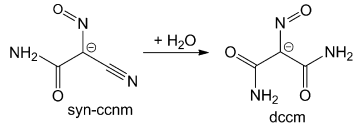	−40.3	−38.0

[a] ΔH_{gas} represents the reaction enthalpy in the gas phase. [b] $\Delta H_{solv} = \Delta H_{gas} + \Delta G_{solv}$ represents the reaction enthalpy in aqueous solution.

not distinguish between the water addition to either of the nitrile groups on the dcnm anion. Being slightly exothermic, the reaction enthalpies of −68 kJ mol^{-1} suggest that the water addition could be kinetically controlled. Thus, kinetic studies were needed to identify whether the addition to one specific nitrile group is more preferred.

TABLE 3: Reaction Barriers in the Gas Phase, $\Delta H^{\ddagger}_{gas}$, and in Water, $\Delta H^{\ddagger}_{solv}$ (in kJ mol^{-1}), of Water Addition Calculated at the MP2/aug-cc-pVTZ Level of Theory

transition state water addition	$\Delta H^{\ddagger}_{gas}$	$\Delta H^{\ddagger}_{solv}$
TS1-1	233.1	242.5
TS1-2	131.6	150.4
TS1-3	95.0	129.8
TS1-NO-1	236.9	244.5
TS1-NO-2	133.9	152.4
TS2	48.4	32.5

Transition States: First Water Addition. The optimized transition state structures are shown in Figure 5, and the reaction barriers calculated at MP2/aug-cc-pVTZ level of theory in the gas phase and in water using the COMSO model are given in Table 3.

Two transition states were found for addition of a water molecule to the first C≡N group to form the *anti* isomer. The first transition state, denoted here as TS1-1, corresponds to the proton transfer from the water molecule to the nitrogen atom, forming the hydroxide anion. The second transition state, denoted here as TS2, corresponds to the addition of this hydroxide anion to the carbon atom of the C≡N group. This is followed by a subsequent molecular rearrangement that leads to the formation of the *anti* isomer. The second step has a relatively low barrier of 48.4 kJ mol^{-1} with the first step, involving proton transfer, having an energy barrier of 233.1 kJ mol^{-1}, and is therefore the rate-controlling step. The solvent effects further favor the second transition state, lowering the corresponding barrier down to 32.5 kJ mol^{-1}, whereas the

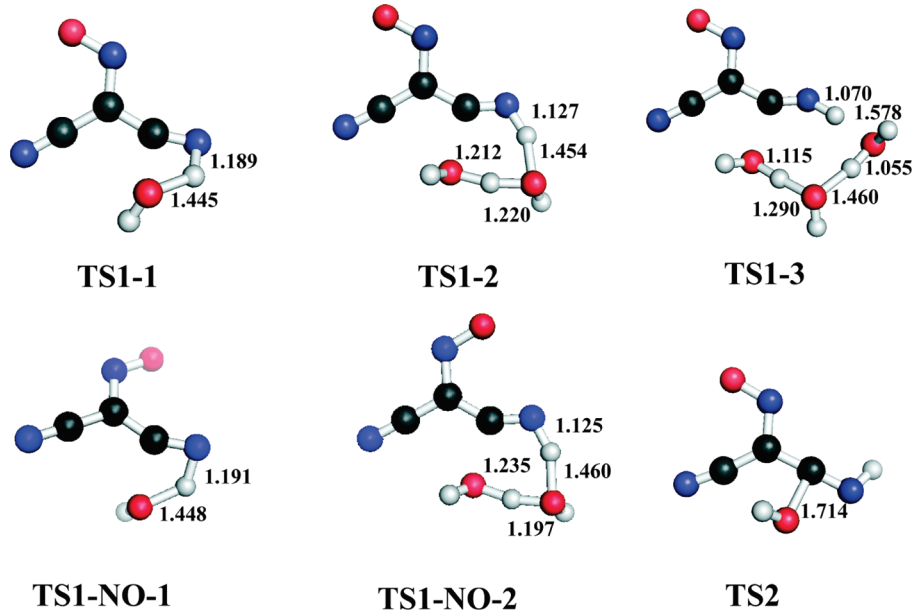

TS1-1 **TS1-2** **TS1-3**

TS1-NO-1 **TS1-NO-2** **TS2**

Figure 5. MP2/aug-cc-pVDZ gas phase optimized structures of the first two transition states for water addition.

reactions barrier for the TS1-1 transition state increases by about 9.4 kJ mol^{-1} to 242.5 kJ mol^{-1}. This is very high for the reaction to be spontaneous and, therefore, less likely to be overcome under ambient conditions, thus making the water addition energetically highly unlikely at room temperature.

A similar mechanism was identified for the addition of HCl to the CN triple bond in alkyl nitriles.[79] The first transition state was also attributed to the proton transfer from the hydrogen chloride molecule to the terminal nitrogen atom that resulted in a significant weakening of the H−Cl bond and thus, the formation of the chloride anion. The barrier calculated at the CI level of theory of 267 kJ mol^{-1} is in good agreement with our theoretical barriers. The reaction barrier of the subsequent addition of the chloride ion was not reported. The authors indicated that in their transition state the Cl−H bond underwent a heterolytic cleavage and the formation of the new C−Cl bond took place after the located transition state.

Recently, it was shown that consideration of a three water chain model was needed to model correctly water addition reactions to the double bonded C═N group in carbodiimines and ketene imines,[80] as the water chain reduced the reaction barriers by about 140 kJ mol^{-1} using a PCM solvent model. It is known that the liquid structure of water consists of hydrogen-bonded water molecules forming an extended three-dimensional network that dynamically changes from random bound and ordered regions to chains and cages. Cooperativity of hydrogen bonding in carboxylic acids is known to make their hydrogen-bonded oligomers stronger acids and thus promotes proton transfer in acid−base mixtures.[81,82] This suggests that a chain of water molecules could act as a stronger proton donor and promote proton transfer. Thus we decided to test whether a chain of strongly hydrogen-bonded water molecules could influence reaction barriers for water addition to the triple bonded C≡N group. The transition states corresponding to the first step of the proton transfer were found when two water molecules (TS1-2) and three water molecules (TS1-3) were included explicitly in the calculations and the corresponding reaction barriers reduced by 101.5 and 138.1 kJ mol^{-1}, respectively. As seen from Figure 5, a chain of water molecules in the TS1-2 and TS1-3 transition states are strongly hydrogen-bonded, with the O−H bonds being elongated in the range of 1.12 to 1.46 Å. This hydrogen-bonded network of water allows for a charge transfer along the chain and hence promotes the proton transfer in the first step of water addition. Inclusion of solvent effects leads to slightly increased reaction barriers of 150.4 and 129.8 kJ mol^{-1} when two and three water molecules are explicitly considered, respectively.

As the reaction barrier decreases with the number of water molecules modeled in the hydrogen-bonded chain the inclusion of more water molecules could potentially further decrease the reaction barrier. However, the relatively high barrier of 129 kJ mol^{-1} indicates that the water addition is rather slow and, therefore, higher temperatures and longer reaction times might be needed to complete the reaction. This outcome is further supported by our experimental findings that only by heating the reaction solution at reflux for 48 h was the quantitative addition of one molecule of water addition to the dcnm anion completed. A ^{13}C NMR spectrum of the reaction solution after heating for only 16 h showed large quantities of the dcnm anion still remaining in solution (Figure S6).

The next step was to investigate if water can add to the nitrile group to form the *syn* isomer. This requires the water addition to the C≡N group that lies in the *cis*-position with respect to the NO group in the dcnm anion. The first transition state, denoted here TS1-NO-1 (see Figure 5), corresponds to the proton transfer and occurs in the same manner as discussed above for the *anti* isomer, with a comparable reaction barrier in water of 244.5 kJ mol^{-1}. Explicit inclusion of a two-water chain resulted in the transition state, denoted here as TS1-NO-2, having a reduced reaction barrier of 152.4 kJ mol^{-1}, which follows the analogous trend found for the *anti* isomer. These findings suggest that the first step of the proton transfer to the nitrogen atom is independent of the position of the NO group with respect to which C≡N group that the water molecule adds. All attempts to find a second transition state for addition of the hydroxide anion formed in the first step to the carbon atom were unsuccessful, possibly influenced by electronic effects, most likely those of orbital symmetry.

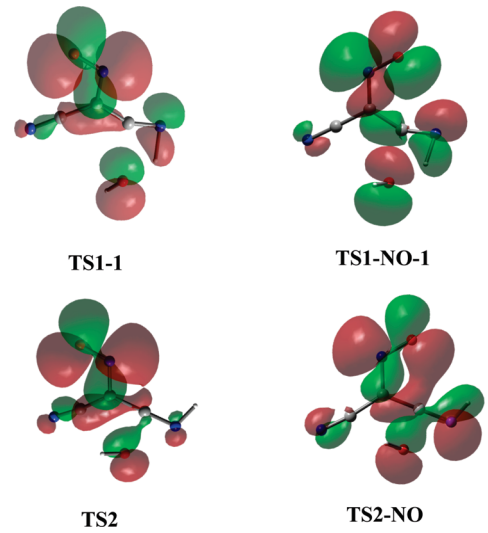

Figure 6. HOMO−1 molecular orbitals in transition states.

To explore these orbital symmetry effects, the HOMO−1 orbital corresponding to the joint π orbital on the hydroxide anion and the nitroso group for both TS1−1 and TS2 were plotted (Figure 6). It can be seen that the π-orbital of the OH anion does not lie in the same plane as the π-orbital of the nitroso group, thus avoiding formation of continuous π-conjugation over the whole molecular system. As a result, the hydroxide anion can interact with one of the π-orbitals on the nitrile group lying in a different plane to that of the nitroso π-orbital and thus add to the carbon atom. A different situation is observed for the transition states TS1-NO-1 and TS2-NO in which water adds to the nitrile group that lies in the *cis*-position to the NO group. Since no genuine second transition state was found, the optimized TS2 structure of the *anti* isomer was taken and the nitroso group was rotated by 180°, thus forming the structure denoted here as TS2-NO. The HOMO−1 molecular orbital was plotted for the TS2-NO structure without a geometry optimization. As seen from Figure 6, the π-orbital of the OH anion now lies in the same plane as that of the NO group, forming continuous π-conjugation over the whole molecular system and preventing the OH anion from interacting with π-orbitals on the nitrile group. The addition of the hydroxide anion to the carbon atom to form *syn*-ccnm is, therefore, forbidden due to orbital symmetry. The theoretical calculations as well as X-ray and NMR measurements support the formation of the preferred *anti*-ccnm anion. It was observed experimentally that a small amount of the *anti* isomer was converted to the *syn* isomer when a pure sample of the *anti*-ccnm anion was left under reflux in H_2O for 48 h. The most likely explanation for this observation is thermally induced rotation of the NO group.

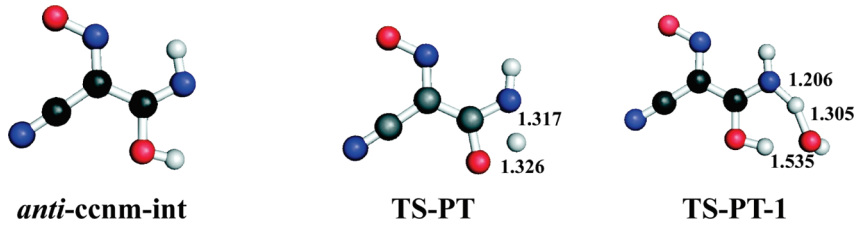

Figure 7. MP2/aug-cc-pVDZ gas phase optimized structures of the intermediate product and the third transition state for water addition.

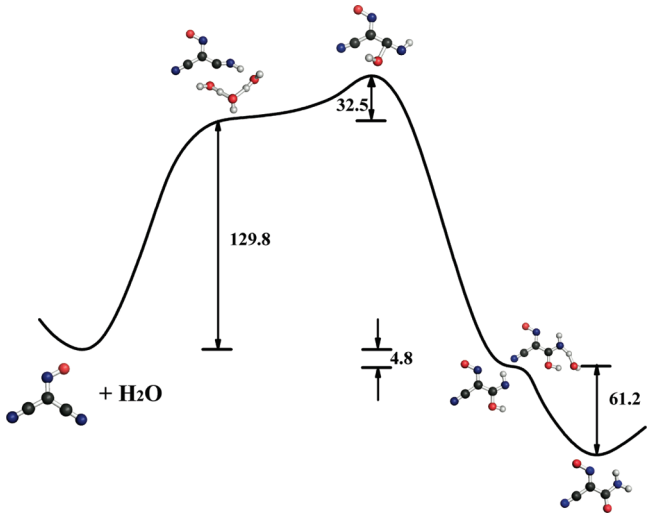

Figure 8. Reaction pathway of water addition to the dcnm anion. The reaction barriers and energies are given in kJ mol^{-1} (as calculated at MP2/aug-cc-pVTZ in combination with the COSMO model).

Once the hydroxide anion is added to the carbon atom, an intermediate product, denoted here as *anti*-ccnm-int, is formed (see Figure 7). This product almost instantaneously undergoes a proton transfer (PT) from the oxygen atom to the =NH group. The transition state, denoted here as TS-PT, was successfully located and is presented in Figure 7. The corresponding barrier as calculated at the MP2/aug-cc-pVTZ level of theory in combination with the COSMO model with respect to the intermediate product, *anti*-ccnm-int, is about 128 kJ mol^{-1}. Explicit inclusion of one water molecule to assist with the proton transfer resulted in a transition state, denoted here as TS-PT-1 and shown in Figure 8, whose reaction barrier was drastically reduced to −6 kJ mol^{-1}, indicating that the proton transfer is basically barrierless in the presence of water molecules and should occur almost instantaneously. The negative reaction barrier is a result of additional stabilization offered by strong hydrogen bonding in the TS. The overall reaction pathway of addition of the first water molecule to the dcnm anion is given in Figure 8.

Second Water Addition. Attempts to add an additional equivalent of water to the ccnm anion to form di(carbamoyl)nitrosomethanide (dccm, $[C(CONH_2)_2(NO)]^-$) using more forceful reaction conditions were unsuccessful. An aqueous solution of (Me_4N)(dcnm) was heated in a microwave reactor to 150 °C for 1.5 h, resulting in the quantitative conversion to (Me_4N)(ccnm) with no indication by ^{13}C NMR spectroscopy of addition of a second equivalent of water. An increase in the reaction temperature to 175 °C resulted in the reaction reaching completion in only 1 h, while a further increase in the reaction temperature to 200 °C for 1.5 h caused degradation of the reactants, with mass spectrometry indicating that only fragments of the starting material remained. Furthermore, the reaction solution had changed from a yellow color, which is highly indicative of the presence of a nitroso group, to nearly colorless, indicating the product had undergone thermal decomposition. The nearly colorless solution also had a distinctive, unpleasant amine odor, which is not characteristic of solutions containing (Me_4N)(dcnm) or (Me_4N)(ccnm).

The lowest energy conformation of the second water addition product is given in Figure 4, and the reaction enthalpies are presented in Table 2. Analysis of these results indicates that the second addition is less exothermic than the first, with the reaction enthalpies decreasing by almost a factor of 2 compared with those of the first addition. If the Evans−Polanyi rule holds for this system,[83] a less exothermic reaction should have higher reaction barriers, thus making the second addition more kinetically controlled. The water addition to the CN triple bond in the *cis*-position to the nitroso group is hindered by orbital symmetry effects. The first step of the water addition, involving the protonation of the terminal nitrogen atom of the C≡N group, for either the *anti*- or *syn*-ccnm anion was found to proceed in the same manner as that for the parental dcnm anion, with similar reaction barriers. Attempts to locate the second transition state of both the *anti*- and *syn*-ccnm anions, corresponding to the addition of the hydroxide anion formed to the carbon atom, were unsuccessful due to the fact that the OH anion preferred to form strong hydrogen bonds with either the carbonyl group or the NO group on the ccnm anion. This finding suggests that the second addition of water to either the *anti*- or *syn*-ccnm anion is likely to be forbidden due to the same electronic effects as described above. This explanation is in good agreement with experiment, as the second addition of water to the *anti*-ccnm anion was not observed even at elevated temperatures of 200 °C.

Methanol Addition. ***First Methanol Addition.*** Under conditions analogous to those that yielded the quantitative conversion of (Me_4N)(dcnm) to (Me_4N)(ccnm), a reaction solution of (Me_4N)(dcnm) dissolved in methanol was heated in the microwave reactor to 150 °C for 1.5 h. ^{13}C NMR spectroscopy showed that this did not result in the formation of cyano(imino(methoxy)methyl)nitrosomethanide (cmnm, $[C(CN)(C(OMe)NH)(NO)]^-$) ions. The reaction was then repeated for 5 h to see if a longer reaction time would give the desired product. Under these conditions ^{13}C NMR spectroscopy indicated that large quantities of the dcnm anion remained in solution but there were also numerous smaller peaks present in the spectrum (Figure S7, Supporting Information). Mass spectrometry performed on the reaction solution revealed not only that the dcnm anion was the predominant species in solution but also that there was a small amount of the cmnm anion present, along with degradation products that could not be identified. When the results of the mass spectrometry and ^{13}C NMR spectroscopy are juxtaposed, it would appear that at 150 °C the addition of methanol to the dcnm anion proceeds very slowly but these aggressive reaction conditions also cause the decomposition of the reactant and product. The decomposition of species in solution is supported by the reaction solution developing a distinctive amine odor, which is normally not present. This

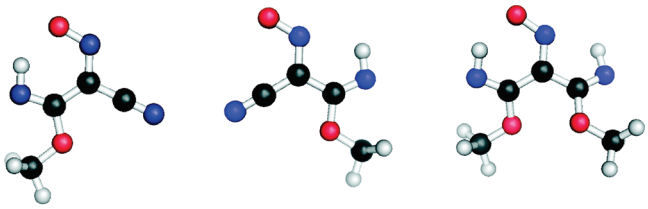

***syn*-cmnm** ***anti*-cmnm** **dmnm**

Figure 9. B3LYP/6-31+G(d) gas phase optimized structures of the methanol addition products (dmnm = di(imino(methoxy)methyl)-nitrosomethanide).

TABLE 4: Reaction Enthalpies (in kJ mol^{-1}) of the Methanol Addition Calculated at the MP2/aug-cc-pVTZ Level of Theory

Reaction	ΔH_{gas}[a]	ΔH_{solv}[b]
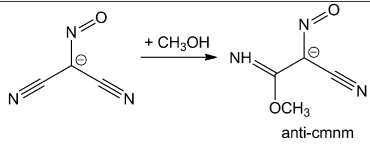 anti-cmnm	−27.6	−33.5
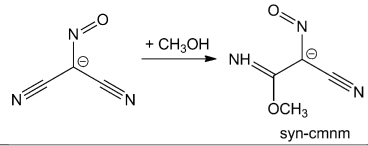 syn-cmnm	−34.5	−33.9
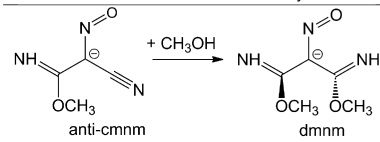 anti-cmnm dmnm	−3.9	1.4
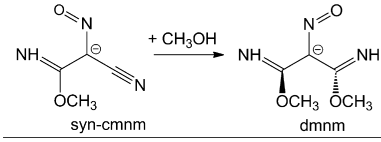 syn-cmnm dmnm	2.8	1.7

[a] ΔH_{gas} represents the reaction enthalpy in the gas phase. [b] $\Delta H_{solv} = \Delta H_{gas} + \Delta G_{solv}$ represents the reaction enthalpy in methanol.

experimental evidence supports the reports in the literature that the addition of alcohols to the dcnm anion only proceeds in the presence of a transition metal cation.[31,33−39]

Optimized geometries of the methanol addition products are shown in Figure 9, and the reaction enthalpies for both steps of methanol addition are presented in Table 4. In the case of the first methanol addition the reaction enthalpies are less exothermic by about 30 kJ mol^{-1} compared to those of water. This indicates that the addition could be again kinetically controlled.

TABLE 5: Reaction Barriers in the Gas Phase, $\Delta H^{\ddagger}_{gas}$, and in Methanol, $\Delta H^{\ddagger}_{solv}$ (in kJ mol^{-1}), of Methanol Addition Calculated at the MP2/aug-cc-pVTZ Level of Theory

transition state methanol addition	$\Delta H^{\ddagger}_{gas}$	$\Delta H^{\ddagger}_{solv}$
TS3-1	191.6	204.0
TS3-2	84.0	112.1
TS3-3	31.1	94.2
TS3-NO-1	202.9	207.5
TS3-NO-2	96.2	124.6
TS4	44.6	31.4

Transition states found for the first nucleophilic addition of methanol are shown in Figure 10 and the corresponding reaction barriers are presented in Table 5. It is expected that due to hyperconjugation, the methyl group should further promote the first step of proton transfer. The calculated reaction barrier for the first transition state, TS3-1, supports this hypothesis. The barrier of 204 kJ mol^{-1} is about 40 kJ mol^{-1} lower than that of the first water addition, TS1-1. Two more transition states were located, denoted here as TS3-2 and TS3-3, when chains comprising two and three hydrogen-bonded methanol molecules, respectively, were explicitly included in the calculations. These two transition states have much lower barriers compared with those for water addition in the gas phase. This suggests that hyperconjugation further increases the strength of hydrogen bonding in a two- or three-molecule methanol chain, thus reducing the reaction barriers. Inclusion of solvent effects leads to an increase in the reaction barriers to 112 kJ mol^{-1} with two methanol molecules and 94 kJ mol^{-1} with three methanol molecules. The latter barrier is 35.6 kJ mol^{-1} lower than that of the analogous transition state, TS1-3, for water addition. Similar barriers of 208 and 125 kJ mol^{-1} were found for the transition states, denoted here as TS3-NO-1 and TS3-NO-2, respectively. As seen from Figure 10, these transition states correspond to one-methanol and two-methanol chained addition to the nitrile arm lying in the *cis*-position to the NO group. The second transition state of methanol addition, TS4, corresponding to the methoxide anion addition to the carbon atom on the nitrile

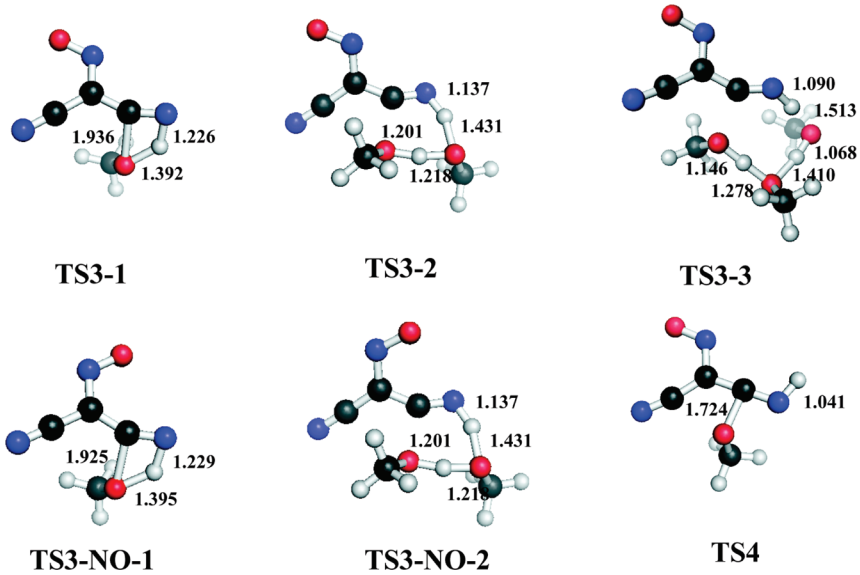

Figure 10. MP2/aug-cc-pVDZ gas phase optimized structures of the transition states for methanol addition.

group has a similar reaction barrier in methanol, compared to that of TS2 in water. These findings indicate that the methanol addition not only should be possible but also occurs faster than water addition.

There seems to be a contradiction with the experimental results, as even elevated temperatures and longer reaction times do not promote methanol addition to the dcnm anion. Many alcohols are known to form linear and cyclic polymer chains in their liquid structure. In recent studies, X-ray and neutron scattering data could be best fitted considering a cyclic hexamer model for methanol.[84,85] Recent molecular dynamics simulations confirmed a significant energetic preference of methanol toward the formation of cyclic oligomers versus linear chains.[86] As the methyl group in methanol offers addition stabilization to the system through hyperconjugation, the hydrogen bonding in the cyclic hexamer is very strong and is calculated to be about 191 kJ mol^{-1} compared with 152 kJ mol^{-1} for a linear hexamer[86] and only 46 kJ mol^{-1} for cyclic hexamers of water.[87] On the basis of these findings, we can conclude that breaking of hydrogen bonds in the cyclic hexamers of methanol is energetically very demanding. Thus, the methanol addition to the nitrile group becomes thermodynamically hindered due to the liquid structure of methanol and as a result only a trace of the addition product was observed in our experiments. It has been shown that the presence of transition metal ions encourages the nucleophilic addition of methanol, which could be attributed to the metal ion either disrupting the cyclic hydrogen-bonded oligomers of methanol or directly interacting with the dcnm anion allowing for the addition to occur through an alternative mechanism, thus encouraging the nucleophilic addition.

Second Methanol Addition. The addition of a second molecule of methanol to the cmnm anion has not been observed, even in the presence of a transition metal ion. The reaction enthalpies calculated in solvent are slightly endothermic, indicating that a thermodynamically unstable product is formed. As shown in Figure 9, the lowest energy confirmation of the addition product, di(imino(methoxy)methyl))nitrosomethanide (dmnm, $[C(C(OMe)NH)_2(NO)]^-$), has two oxygen atoms in close proximity to each other that causes them to repel, thus forcing the oxygen atoms out of the plane by 40° and disrupting the overall π-conjugation in the anion. This steric hindrance due to geometric constraints in the cmnm anion hinders the methanol addition thermodynamically such that even the presence of transition metal cations, which greatly increases the rate of the addition of methanol to a nitrile group of the dcnm anion, does not encourage the formation of the dmnm anion, even under solvothermal reaction conditions.[31]

Conclusions

Experimentally the addition of 1 equiv of water to the dcnm anion was observed to be complete after 48 h at reflux, with both the *syn* and *anti* isomers of the ccnm anion observed in the product. Thermodynamically, the formation of both *anti* and *syn* isomers is equally possible, but *ab initio* calculations indicate that formation of the *syn*-ccnm is prohibited due to electronic effects on the mechanism and its formation can be attributed to rotation of the NO group in *anti*-ccnm. The water addition to the CN group was found to go through three distinct transition states: (1) the transfer of a proton from a water molecule to the nitrile group, (2) the subsequent attack of the generated hydroxide anion on the carbon atom of the nitrile group, and (3) a rapid proton transfer to form a carbamoyl group. The first step is the rate-limiting step and is facilitated by a chain of hydrogen-bonded water molecules allowing for a charge transfer along the chain, thereby reducing the reaction barrier to 129 kJ mol^{-1} when a chain of three water molecules was considered, in comparison to 242.5 kJ mol^{-1} when no hydrogen bonded water molecule chain was modeled. Although the reaction barrier reduces significantly with multiple water molecules present, it is still relatively high for the reaction to be spontaneous, therefore requiring elevated temperatures and long reaction times to achieve a complete conversion of the dcnm anion to the *anti*-ccnm anion. Water addition to the nitrile group lying in the *cis*-position to the nitroso group is hindered by orbital symmetry effects, and therefore, the formation of the *syn* isomer could only be attributed to the rotation of the nitroso group from the *anti*-ccnm anion. This finding, in turn, prevents the second addition of water to the *anti*-ccnm anion. The NO group rotation was found to be energetically demanding, with the barrier being around 155 kJ mol^{-1} in both the parent dcnm anion and *anti*-ccnm anion. Therefore, the rotation does not occur readily at room temperature, which would give the distinct ^{13}C peaks corresponding to *anti*- and *syn*-ccnm anions in the NMR measurements. Due to the high barrier, the nitroso rotation is restricted and can only occur to a small extent, accounting for the limited *anti* to *syn* isomeric conversion observed upon heating the *anti*-ccnm anion.

Addition of a methanol molecule to dcnm was not observed experimentally, even at 150 °C. According to our calculations of the first transition state of the proton transfer a three-methanol chain should facilitate the addition by reducing the barrier to 94 kJ mol^{-1}, which is lower than that of the first transition state of water addition. However, as shown by previous studies, methanol is more likely to exist as cyclic hexamers that are strongly hydrogen-bonded, thus hindering formation of linear methanol chains and retarding the nucleophilic addition of methanol to the nitrile group. As a result, the first addition of methanol can be facilitated only by the presence of transition metal ions. The second methanol addition is not observed experimentally, regardless of the presence of transition metal ions. The calculated reaction enthalpies of the second methanol addition are slightly endothermic, indicating that a thermodynamically unstable product is formed having two oxygen atoms repelling each other due to unavoidable geometric constraints.

Acknowledgment. We gratefully acknowledge generous allocations of computing time from the National Facility of the National Computational Infrastructure (Canberra, Australia) and the Monash Sun Grid Cluster at the e-research centre of Monash University, Australia. We thank the Australian Research Council for funding Discovery grants to S.R.B. and G.B.D. and for Australian Postdoctoral Fellowships (E.I.I. and D.R.T.), and the Australian Institute of Nuclear Science and Engineering for financial support (D.R.T., A.S.R.C.). A.S.R.C. also acknowledges an Australian Postgraduate Award scholarship.

Supporting Information Available: ^{13}C NMR spectra of (Me_4N)(ccnm) and (Me_4N)(dcnm) (Figure S1−S7). NBO analysis of dcnm and *anti*- and *syn*-ccnm anions (Table S1). Optimized geometries of all the species studied here in the form of the GAUSSIAN archive files (see Tables S2 and S3). The CIF may be obtained free of charge from The Cambridge Crystallographic Data Centre via www.ccdc.cam.ac.uk/data_request/cif. CCDC reference number 783466. This material is available free of charge via the Internet at http://pubs.acs.org.

References and Notes

(1) Batten, S. R.; Murray, K. S. *Coord. Chem. Rev.* **2003**, *246*, 103–130.

(2) Forsyth, S. A.; Batten, S. R.; Dai, Q.; MacFarlane, D. R. *Aust. J. Chem.* **2004**, *57*, 121–124.
(3) Dai, Q.; Menzies, D. B.; MacFarlane, D. R.; Batten, S. R.; Forsyth, S.; Spiccia, L.; Cheng, Y.-B.; Forsyth, M. *C. R. Chimie* **2006**, *9*, 617–621.
(4) Arras, J.; Steffan, M.; Shayeghi, Y.; Ruppert, D.; Claus, P. *Green Chem.* **2009**, *11*, 716–723.
(5) MacFarlane, D. R.; Forsyth, S. A.; Golding, J.; Deacon, G. B. *Green Chem.* **2002**, *4*, 444–448.
(6) MacFarlane, D. R.; Golding, J.; Forsyth, S.; Forsyth, M.; Deacon, G. B. *Chem. Commun.* **2001**, 1430–1431.
(7) Kulkarni, P. S.; Branco, L. C.; Crespo, J. G.; Nunes, M. C.; Raymundo, A.; Afonso, C. A. M. *Chem.—Eur. J.* **2007**, *13*, 8478–8488.
(8) Gerhard, D.; Alpaslan, S. C.; Gores, H. J.; Uerdingenc, M.; Wasserscheid, P. *Chem. Commun.* **2005**, 5080–5082.
(9) Forsyth, S. A.; MacFarlane, D. R.; Thomson, R. J.; Itzstein, M. v. *Chem. Commun.* **2002**, 714–715.
(10) Zhang, Q.; Liu, S.; Li, Z.; Li, J.; Chen, Z.; Wang, R.; Lu, L.; Deng, Y. *Chem.—Eur. J.* **2009**, *15*, 765–778.
(11) Yoshida, Y.; Muroi, K.; Otsuka, A.; Saito, G.; Takahashi, M.; Yoko, T. *Inorg. Chem.* **2004**, *43*, 1458–1462.
(12) Wooster, T. J.; Johanson, K. M.; Fraser, K. J.; MacFarlane, D. R.; Scott, J. L. *Green Chem.* **2006**, *8*, 691–696.
(13) Wang, P.; Wenger, B.; Humphry-Baker, R.; Moser, J.-E.; Teuscher, J.; Kantlehner, W.; Mezger, J.; Stoyanov, E. V.; Zakeeruddin, S. M.; Grätzel, M. *J. Am. Chem. Soc.* **2005**, *127*, 6850–6856.
(14) Mazille, F.; Fei, Z.; Kuang, D.; Zhao, D.; Zakeeruddin, S. M.; Grätzel, M.; Dyson, P. J. *Inorg. Chem.* **2006**, *45*, 1585–1590.
(15) Brand, H.; Liebman, J. F.; Schulz, A.; Mayer, P.; Villinger, A. *Eur. J. Inorg. Chem.* **2006**, 4294–4308.
(16) Brand, H.; Mayer, P.; Polborn, K.; Schulz, A.; Weigand, J. J. *J. Am. Chem. Soc.* **2005**, *127*, 1360–1361.
(17) Brand, H.; Mayer, P.; Schulz, A.; Weigand, J. J. *Angew. Chem., Int. Ed.* **2005**, *44*, 3929–3932.
(18) Brand, H.; Schulz, A.; Villinger, A. *Z. Anorg. Allg. Chem.* **2007**, *633*, 22–35.
(19) Izgorodina, E. I.; Forsyth, M.; MacFarlane, D. R. *Aust. J. Chem.* **2007**, *60*, 15–20.
(20) Rembarz, G.; Fischer, E.; Röber, K.-C.; Ohff, R.; Crahmer, H. *J. Prakt. Chem.* **1969**, *311*, 889–892.
(21) Igashira-Kamiyama, A.; Kajiwara, T.; Konno, T.; Ito, T. *Inorg. Chem.* **2006**, *45*, 6460–6466.
(22) Zheng, L.-L.; Leng, J.-D.; Liu, W.-T.; Zhang, W.-X.; Lu, J.-X.; Tong, M.-L. *Eur. J. Inorg. Chem.* **2008**, *29*, 4616–4624.
(23) Hvastijová, M.; Kohout, J. *Z. Anorg. Allg. Chem.* **1991**, *600*, 177–180.
(24) Hvastijová, M.; Kohout, J.; Köhler, H.; Ondrejovič, G. *Z. Anorg. Allg. Chem.* **1988**, *566*, 111–120.
(25) Bjernemose, J. K.; McKenzie, C. J.; Raithby, P. R.; Teat, S. J. *Dalton Trans.* **2003**, 2639–2640.
(26) Turner, D. R.; Pek, S. N.; Cashion, J. D.; Moubaraki, B.; Murray, K. S.; Batten, S. R. *Dalton Trans.* **2008**, 6877–6879.
(27) Longo, G. *Gazz. Chem. Ital.* **1931**, *61*, 575.
(28) Chesman, A. S. R.; Turner, D. R.; Izgorodina, E. I.; Batten, S. R.; Deacon, G. B. *Dalton Trans.* **2007**, 1371–1373.
(29) Bohle, D. S.; Conklin, B. J.; Hung, C.-H. *Inorg. Chem.* **1995**, *34*, 2569–2581.
(30) Price, D. J.; Batten, S. R.; Berry, K. J.; Moubaraki, B.; Murray, K. S. *Polyhedron* **2003**, *22*, 165–176.
(31) Chesman, A. S. R.; Turner, D. R.; Price, D. J.; Moubaraki, B.; Murray, K. S.; Deacon, G. B.; Batten, S. R. *Chem. Commun.* **2007**, 3541–3543.
(32) Köhler, H.; Seifert, B. *Z. Anorg. Allg. Chem.* **1970**, *379*, 1–8.
(33) Hvastijová, M.; Kohout, J.; Buchler, J. W.; Boča, R.; Koíšek, J.; Jäger, L. *Coord. Chem. Rev.* **1998**, *175*, 17–42.
(34) Dunaj-Jurčo, M.; Mikloš, D.; Potočňák, I.; Jäger, L. *Acta Crystallogr. Sect. C* **1996**, *C52*, 2409–2412.
(35) Dunaj-Jurčo, M.; Mikloš, D.; Potočňák, I.; Jäger, L. *Acta Crystallogr. Sect. C* **1998**, *C54*, 1763–1765.
(36) Buchler, J. W.; Hvastijová, M.; Kohout, J.; Kožíšek, J. *Trans. Met. Chem.* **1998**, *23*, 215–220.
(37) Hvastijová, M.; Kohout, J.; Kožíšek, J.; Svoboda, I. *J. Coord. Chem.* **1999**, *47*, 573–579.
(38) Hvastijová, M.; Kožíšek, J.; Kohout, J. *J. Coord. Chem.* **1995**, *36*, 195–205.
(39) Hvastijová, M.; Kožíšek, J.; Kohout, J.; Díaz, J. G. *Inorg. Chim. Acta* **1995**, *236*, 163–165.
(40) Chesman, A. S. R.; Turner, D. R.; Deacon, G. B.; Batten, S. R. *Chem. Asian J.* **2009**, *4*, 761–769.
(41) Arulsamy, N.; Bohle, D. *J. Org. Chem.* **2000**, *65*, 1139–1143.
(42) Taylor, E. C.; Vogl, O.; Cheng, C. C. *J. Am. Chem. Soc.* **1959**, *81*, 2442–2448.
(43) Vogl, O.; Taylor, E. C. *J. Am. Chem. Soc.* **1957**, *79*, 518–519.
(44) Chesman, A. S. R.; Turner, D. R.; Deacon, G. B.; Batten, S. R. *Eur. J. Inorg. Chem.* **2010**, *18*, 2798–2812.
(45) Gerasimchuk, N.; Goeden, L.; Durham, P.; Barnes, C.; Cannon, J. F.; Silchenko, S.; Hidalgo, I. *Inorg. Chim. Acta* **2008**, *361*, 1983–2001.
(46) Mokhir, A. A.; Domasevich, K. V.; Dalley, N. K.; Kou, X.; Gerasimchuk, N. N.; Gerasimchuk, O. A. *Inorg. Chim. Acta* **1999**, *284*, 85–98.
(47) Ponomareva, V. V.; Dalley, N. K.; Kou, X.; Gerasimchuk, N. N.; Domasevitch, K. V. *J. Chem. Soc., Dalton Trans.* **1996**, 2351–2359.
(48) Domasevitch, K. V.; Gerasimchuk, N. N.; Mokhir, A. *Inorg. Chem.* **2000**, *39*, 1227–1237.
(49) Eddings, D.; Barnes, C.; Gerasimchuk, N.; Durham, P.; Domasevich, K. *Inorg. Chem.* **2004**, *43*, 3894–3909.
(50) Gerasimchuk, N.; Maher, T.; Durham, P.; Domasevitch, K. V.; Wilking, J.; Mokhir, A. *Inorg. Chem.* **2007**, *46*, 7268–7284.
(51) Nakamura, H.; Iitaka, Y.; Sakakibara, H.; Umezawa, H. *J. Antibiot.* **1974**, *27*, 894–896.
(52) Sakakibara, H.; Naganawa, H.; Ohno, M.; Maeda, K.; Umezawa, H. *J. Antibiot.* **1974**, *27*, 897–899.
(53) Brand, H.; Liebman, J. F.; Schulz, A. *Eur. J. Org. Chem.* **2008**, 4665–4675.
(54) Chesman, A. S. R.; Turner, D. R.; Moubaraki, B.; Murray, K. S.; Deacon, G. B.; Batten, S. R. *Chem.—Eur. J.* **2009**, *15*, 5203–5207.
(55) Otwinowski, Z.; Minor, W. *Methods Enzymology*; Academic Press: New York NY, U.S., 1997; Vol. 276.
(56) Sheldrick, G. M. *Acta Crystallogr.* **2008**, *A64*, 112–122.
(57) Barbour, L. J. *J. Supramol. Chem.* **2001**, *1*, 189–191.
(58) Frischt, M. J. Trucks, G. W.; Schlegel, H. B.; Scuseria, G. E.; Robb, M. A.; Cheeseman, J. R. ; Montgomery, J. A., Jr.; Kudin, K. N.; Burant, J. C.; Millam, J. M.; Iyengar, S. S.; Tomasi, J.; Barone, V.; Mennucci, B.; Cossi, M.; Scalmani, G.; Rega, N.; Petersson, G. A.; Nakatsuji, H.; Hada, M.; Ehara, M.; Toyota, K.; Fukuda, R.; Hasegawa, J.; Ishida, M.; Nakajima, T.; Honda, Y.; Kitao, O.; Nakai, H.; Klene, M.; Li, X.; Knox, J. E.; Hratchian, H. P.; Cross, J. B.; Bakken, V.; Adamo, C.; Jaramillo, J.; Gomperts, R.; Stratmann, R. E.; Yazyev, O.; Austin, A. J.; Cammi, R.; Pomelli, C.; Ochterski, J. W.; Ayala, P. Y.; Morokuma, K.; Voth, G. A.; Salvador, P.; Dannenberg, J. J.; Zakrzewski, V. G.; Dapprich, S.; Daniels, A. D.; Strain, M. C.; Farkas, O.; Malick, D. K.; Rabuck, A. D.; Raghavachari, K.; Foresman, J. B.; Ortiz, J. V.; Cui, Q.; Baboul, A. G.; Clifford, S.; Cioslowski, J.; Stefanov, B. B.; G. Liu, A. L.; Piskorz, P.; Komaromi, I.; Martin, R. L.; Fox, D. J.; Keith, T.; Al-Laham, M. A.; Peng, C. Y.; Nanayakkara, A.; Challacombe, M.; Gill, P. M. W.; Johnson, B.; Chen, W.; Wong, M. W.; Gonzalez, C.; Pople, J. A. *GAUSSIAN 09*, Revision A.02; Gaussian, Inc.: Wallingford, CT, U.S., 2009.
(59) Baerends, E. J. ; Autschbach, J.; Berger, J. A.; Bérces, A.; Bickelhaupt, F. M.; Bo, C.; de Boeij, P. L. ; Cavallo, L.; Chong, D. P.; Deng, L.; Dickson, R. M.; Ellis, D. E.; van Faassen, M. L.; Fan, L.; Fischer, T. H.; Fonseca Guerra, C.; van Gisbergen, S. J. A.; Götz, A. W.; Groeneveld, J. A.; Gritsenko, O. V.; Grüning, M.; Harris, F. E.; van den Hoek, P.; Jacob, C. R.; Jacobsen, H. Jensen, L.; Kadantsev, E. S.; van Kessel, G.; Klooster, R.; Kootstra, F.; Krykunov, M. V.; van Lenthe, E.; Louwen, J. N.; McCormack, D. A.; Michalak, A.; Neugebauer, J.; Nicu, V. P.; Osinga, V. P.; Patchkovskii, A.; Philipsen, P. H. T.; Post, D.; Pye, C. C.; Ravenek, W.; Rodriguez, J. I.; Romaniello, P.; Ros, P. Schipper, P. R. T.; Schreckenbach, G.; Snijders, J. G.; Solà, M.; Swart, M.; Swerhone, D.; te Velde, G.; Vernooijs, P.; Versluis, L.; Visscher, L.; Visser, O.; Wang, T.; Wesolowski, T. A.; van Wezenbeek, E. M.; Wiesenekker, G.; Wolff, S. K.; Woo, T. K.; Yakovlev, A. L.; Ziegler, T. *ADF 2009 01b; Scientific Computing & Modelling NV (SCM)*.
(60) Becke, A. D. *J. Chem. Phys.* **1992**, *96*, 5648–5652.
(61) Lee, C.; Yang, W.; Pass, R. G. *Phys. Rev. B* **1988**, *37*, 785–789.
(62) Francl, M. M.; Pietro, W. J.; Hehre, W. J.; Binkley, J. S.; DeFrees, D. J.; Pople, J. A.; Gordon, M. S. *J. Chem. Phys.* **1982**, *77*, 3654–3665.
(63) Ditchfield, R.; Hehre, W. J.; Pople, J. A. *J. Chem. Phys.* **1971**, *54*, 724–728.
(64) Purvis, G. D.; Bartlett, R. J. *J. Chem. Phys.* **1982**, *76*, 1910–1918.
(65) Dunning, T. H., Jr. *J. Chem. Phys.* **1989**, *90*, 1007–1023.
(66) Kendall, R. A.; Dunning, T. H., Jr.; Harrison, R. J. *J. Chem. Phys.* **1992**, *96*, 6769–6806.
(67) Helgaker, T.; Jørgensen, P.; Olsen, J. *Molecular Electronic-Structure Theory*; John Wiley and Sons Ltd.: New York, NY, U.S., 2000.
(68) Head-Gordon, M.; Pople, J. A.; Frisch, M. J. *Chem. Phys. Lett.* **1988**, *153*, 503–506.
(69) MØller, C.; Plesset, M. S. *Phys. Rev.* **1934**, *46*, 618–622.
(70) Klamt, A. *COSMO-RS, From Quantum Chemistry to Fluid Phase Thermodynamics and Drug Design*; Elsevier: Amsterdam, The Netherlands, 2005.
(71) Klamt, A.; Eckert, F.; Diedenhofen, M.; Beck, M. E. *J. Phys. Chem. A* **2003**, *107*, 9380–9386.
(72) Tomasi, J.; Persico, M. *Chem. Rev.* **1994**, *94*, 2027–2094.
(73) Ditchfield, R. *Mol. Phys.* **1974**, *27*, 789–807.
(74) Wolinski, K.; Hilton, J. F.; Pulay, P. *J. Am. Chem. Soc.* **1990**, *112*, 8251–8260.

(75) Foster, J. P.; Weinhold, F. *J. Am. Chem. Soc.* **1980**, *102*, 7211–7218.
(76) Reed, A. E.; Weinstock, R. B.; Weinhold, F. *J. Chem. Phys.* **1985**, *83*, 735–746.
(77) Roohi, H.; Deyhimi, F.; Ebrahimi, A.; Khanmohammady, A. *J. Mol. Struct. (THEOCHEM)* **2005**, *718*, 123–132.
(78) Roohi, H.; Deyhimi, F.; Ebrahimi, A. *J. Mol. Struct. (THEOCHEM)* **2001**, *543*, 299–308.
(79) Alagona, G.; Tomasi, J. *THEOCHEM* **1983**, *91*, 263–281.
(80) Nguyen, M. T.; Raspoet, G.; Vanquickenborne, L. G. *J. Chem. Soc., Perkin Trans. 2* **1999**, 813–820.
(81) Johansson, K.; Izgorodina, E. I.; Forsyth, M.; MacFarlane, D. R. *Phys. Chem. Chem. Phys.* **2008**, *10*, 2972–2978.
(82) *Theoretical treatments of hydrogen bonding*; Hadzi, D. , Ed.; John Wiley & Sons: New York, NY, U.S., 1997.
(83) Evans, M. G. *Discuss. Faraday Soc.* **1947**, *2*, 271–279.
(84) Sarkar, S.; Joarder, R. N. *J. Chem. Phys.* **1993**, *99*, 2032–2039.
(85) Sarkar, S.; Joarder, R. N. *J. Chem. Phys.* **1994**, *100*, 5118–5122.
(86) Ludwig, R. *ChemPhysChem* **2005**, *6*, 1369–1375.
(87) Goldman, N.; Leforestier, C.; Saykally, R. J. *Phil. Trans. R. Soc. A* **2005**, *363*, 493–508.

JP108550Z